JPE Journal of Photonics for Energy

RESEARCH PAPER

Hot electrons and cold holes: operation, efficiency, and design of a two-temperature hot-carrier solar cell

Thomas Vezin, Nathan Roubinowitz, Jean-François Guillemoles, and Daniel Suchet*

Institut Photovoltaique d'Ile de France, UMR-IPVF 9006, CNRS, Ecole Polytechnique IPP, ENSCP PSL, Palaiseau, France

ABSTRACT. Hot-carrier solar cells (HCSCs) offer the potential to enhance the energy-conversion efficiency of photovoltaic devices up to 86%. However, most HCSC models to date assume that electrons and holes have the same temperature, whereas many reports in III to V materials indicate that electrons can be much hotter than their counterparts. We present a detailed balance HCSC model that includes different temperatures for electrons and holes. We focus on the impact of the temperature imbalance on the voltage of such an HCSC and its power-conversion efficiency. Surprisingly, a temperature imbalance at a fixed effective temperature leads to a slight power-conversion efficiency increase, up to 1 to 2 percentage points, primarily due to an increase in fill factor and possibly open-circuit voltage. Yet, we show that the knowledge of the effective temperature alone is sufficient to design a satisfying HCSC.

Keywords: hot-carrier solar cells; two-temperature; simulation; efficiency; voltage

Paper 24051SS received Oct. 1, 2024; revised Jan. 30, 2025; accepted Feb. 12, 2025; published Mar. 7, 2025.

1 Introduction

Hot-carrier solar cells (HCSCs) are photovoltaic devices designed to take advantage of the slow energy relaxation rate of photogenerated carriers to achieve efficiencies exceeding the usual limit for conventional systems. In steady-state operation, these devices are characterized by carrier distributions at temperatures higher than that of the surrounding lattice. Adequately designed energy-selective contact (ESC) then converts this temperature increase into a voltage boost, allowing theoretically power-conversion efficiencies up to 86%.[1,2]

Since the initial work of Ross and Nozik, most studies devoted to HCSCs have considered both electrons and holes to share a single temperature $T > T_{\text{lattice}}$. Electron–hole interactions indeed tend to equate the temperatures of both distributions. However, many other processes can lead *a contrario* to a temperature difference. Upon photogeneration, the energy of the absorbed photon is distributed between electrons and holes according to their effective masses, and electrons promoted to the conduction band usually receive more power than their heavier hole counterparts. The cooling rate, which relies on carrier–phonon interactions, may also be different for electrons and holes because the coupling to phonon modes depends on the dispersion relation. If these processes are stronger than the interband interactions, the steady-state temperatures of electrons and holes will be different.

*Address all correspondence to Daniel Suchet, daniel.suchet@polytechnique.edu

1947-7988/2025/$28.00 © 2025 SPIE

The radiative emission of such a two-temperature (2T) system has been shown to resemble the generalized Planck law of radiation[3] with an effective temperature and chemical potential.[4] Building on this theoretical analysis, the first direct experimental signature of such a 2T distribution was recently reported in an InGaAsP quantum well absorber.[5]

This work investigates the impact of $T_e \neq T_h$ not only on the radiative emission of the absorber but also on the operation of the HCSC. Compared with a usual HCSC operating at 2000 K, how would the system perform if electrons were slightly hotter and holes slightly colder? A previous study[6] used a detailed balance model to investigate numerically the influence of several parameters on the performance of a 2T HCSC device, with a strong focus on the behavior of semi-selective energy selective contacts. Following a similar approach with simplified assumptions, this work offers a better understanding of the impact of the 2T effect on the performances of an HCSC. In particular, the expression of the voltage at the terminals of a 2T HCSC is derived analytically and compared with the monothermal (1T) reference case. Finally, the effective temperature is shown to be the key parameter governing the operation of a 2T HCSC and thus the critical quantity to design its contacts.

2 Detailed Balance Model for a Two-Temperature Hot-Carrier Solar Cell

Conventional solar cells have been successfully described by a detailed balance model accounting for carrier generation and recombination.[7,8] In the context of hot-carrier solar cells, this model has been expanded to include power balance.[1,6,9,10] In this section, the main lines of the model are recalled and adapted to the case of uneven electron and hole temperatures. The model is graphically summarized in Fig. 1.

2.1 Optoelectronic Processes

Electrons (resp. holes) are assumed to form a thermal distribution with a temperature T_e (resp. T_h) and a chemical potential μ_e (resp. μ_h) (see Appendix A for the sign convention). The temperature ratio will be noted $r = T_e/T_h$, and a 2T HCSC is characterized by $r \neq 1$.

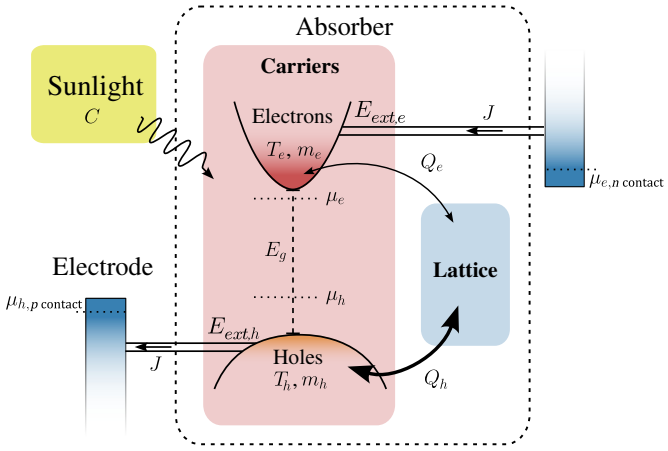

Fig. 1 Schematic representation of the simulated 2T HCSC. The absorbing material is parametrized with its energy gap E_g, the effective masses of electrons (m_e) and holes (m_h) and the thermalization rates for both carriers (Q_e and Q_h). The energy-selective contacts are parametrized with their extraction energies ($E_{\text{ext,e}}$ and $E_{\text{ext,h}}$). The solar illumination is parametrized with a concentration factor C. Carrier distributions are characterized by their temperatures and chemical potentials.

2.1.1 *Photogeneration*

The absorber is illuminated the solar radiation, described as blackbody radiation. The spectral density of photon flux reaching the absorber is

$$\phi_{\odot}(C,E) = C\sin^2(\theta_{\odot}) \times \frac{2\pi}{h^3c^2}E^2\left(\exp\left(\frac{E}{k_BT_{\odot}}\right)-1\right)^{-1}, \tag{1}$$

where $T_{\odot} = 5778$ K is the temperature of the surface of the Sun, $2\theta_{\odot} = 32'$ is the angular diameter of the Sun seen from the Earth, and $1 < C < \sin^{-2}(\theta_{\odot}) \simeq 46{,}000$ is the concentration factor.[11] The total power reaching the device is thus

$$P_{\odot}(C) = \int_0^{\infty} \phi_{\odot}(C,E)\mathrm{d}E. \tag{2}$$

Following the same simplifying assumption as Shockley and Queisser and Ross and Nozik, the absorptivity of the system is assumed to be a step-like function $A(E) = \Theta(E - E_g)$, where E_g is the gap of the absorber. The photon flux absorbed by the system is

$$\Phi_{\mathrm{abs}}(C,E_g) = \int_{E_g}^{\infty} \phi_{\odot}(C,E)\mathrm{d}E. \tag{3}$$

Because each photon generates an electron and a hole at the same time, the generation rate of both carriers is equal, but the absorbed power is not. In the effective mass approximation, when a photon of energy E is absorbed, its energy is distributed within the photo-generated electron–hole pair as[6]

$$\begin{cases} E_e = E_g/2 + (1-\xi)(E-E_g) \\ E_h = E_g/2 + \xi(E-E_g) \end{cases}, \tag{4}$$

where $\xi = m_e/(m_e + m_h)$ is the effective mass mismatch. The power $P_{\mathrm{abs,i}}$ received by the population $i = e, h$ is thus

$$P_{\mathrm{abs,i}} = \int_{E_g}^{\infty} E_i\phi_{\odot}(C,E)\mathrm{d}E. \tag{5}$$

2.1.2 *Carrier recombination*

Following Kirchhoff's law, an absorbing system will necessarily emit radiation. In the context of a 2T system, the radiative emission has been shown to be[4]

$$\Phi_{\mathrm{rad}}(E) = A(E)\frac{2\pi}{h^3c^2}E^2\left(\exp\left(\frac{E-\Delta\mu_{\mathrm{eff}}}{k_BT_{\mathrm{eff}}}-1\right)\right)^{-1}, \tag{6}$$

where the effective temperature T_{eff} and effective quasi-Fermi-level splitting (QFLS) $\Delta\mu_{\mathrm{eff}}$ are related to the carrier temperatures T_e, T_h and chemical potentials μ_e, μ_h

$$\begin{cases} \frac{1}{T_{\mathrm{eff}}} = \frac{1-\xi}{T_e} + \frac{\xi}{T_h} \\ \frac{\Delta\mu_{\mathrm{eff}}}{k_BT_{\mathrm{eff}}} = \frac{\mu_e}{k_BT_e} + \frac{\mu_h}{k_BT_h} - \frac{E_g}{k_B}\left(\frac{1}{2}-\xi\right)\left(\frac{1}{T_h}-\frac{1}{T_e}\right) \end{cases}. \tag{7}$$

In the following, the Bose–Einstein distribution of the previous equation will be approximated by a Maxwell–Boltzmann distribution.

Similar to the absorption process, the emitted energy is unevenly distributed between electrons and holes. Radiative emission draws from population i a power

$$P_{\mathrm{rad,i}} = \int_{E_g}^{\infty} E_i \times \Phi_{\mathrm{rad}}(E)\mathrm{d}E. \tag{8}$$

For the sake of simplicity, the analysis is restricted to the radiative limit, and other recombination processes are neglected.

2.1.3 *Carrier thermalization*

Through their interaction with the surrounding lattice, carriers dissipate their excess of kinetic energy and their distributions relax toward ambient temperature. This cooling process has been described phenomenologically by a linear power dissipation parametrized by a thermalization coefficient Q.[10,12,13] In the context of a 2T system, electrons and holes may have different thermalization coefficients,[6] and the previous model can be generalized to

$$P_{\text{th,i}} = Q_i(T_i - T_{\text{lattice}}), \tag{9}$$

where $P_{\text{th,i}}$ is the power thermalized by carriers i, and Q_i is the thermalization coefficient of carriers i.

2.1.4 *Carriers extraction*

Finally, carriers will be extracted through the energy-selective contacts. Compared with Ref. 6, contacts are here assumed to be mono-energetic at energy $E_{\text{ext,e}}$ for electrons and $E_{\text{ext,h}}$ for holes. When an electrical current J flows from the absorber toward the terminals, carriers i loose a power

$$P_{\text{ext,i}} = \frac{J}{e} \times E_{\text{ext,i}}, \tag{10}$$

where e is the elementary charge.

In the following, $E_{\text{ext}} = E_{\text{ext,e}} + E_{\text{ext,h}}$ is the extraction energy of the electron–hole pairs (see Appendix A for the sign convention).

2.2 Balance Equations

The thermodynamical state of the 2T HCSC is described by four parameters (T_e, μ_e, T_h, μ_h). These quantities are related through the electro-neutrality condition. Assuming that the density of photogenerated carriers is large compared with the density of charged impurities and within Boltzmann approximation, this condition provides an explicit relation[6]

$$\frac{\mu_e}{T_e} = \frac{\mu_h}{T_h} + k_B \frac{D}{2} \ln\left(\frac{m_h T_h}{m_e T_e}\right) - \frac{E_g}{2}\left(\frac{1}{T_h} - \frac{1}{T_e}\right), \tag{11}$$

where D is the dimensionality of the absorber ($D = 3$ in this work).

To compute it at a given operation point (i.e., given value of the current), four equations are therefore needed. Three of them are provided by the detailed balance particle and energy flows as in

$$\begin{cases} \Phi_{\text{abs}} = \Phi_{\text{rad}} + \frac{J}{e} \\ P_{\text{abs,e}} = P_{\text{rad,e}} + P_{\text{th,e}} + P_{\text{ext,e}} \\ P_{\text{abs,h}} = P_{\text{rad,h}} + P_{\text{th,h}} + P_{\text{ext,h}} \end{cases}. \tag{12}$$

2.3 Monothermal Limit

This model generalizes previous models for 1T HCSCs,[10,14] and the behavior of 1T HCSCs can be recovered as a limit case, which will be used as reference.

The 1T case corresponds to a situation where electrons and holes share the same temperature at all operating points of the device (but this temperature may vary with the operating point). This relation sets constraints on the absorber properties (Q_e and Q_h) and on the contact designs ($E_{\text{ext,e}}$ and $E_{\text{ext,h}}$).

At open-circuit voltage (i.e., $J = 0$), electrons and holes will share the same temperature if and only if their thermalization coefficients compensate for the energy imbalance of radiative processes

$$\frac{Q_e}{Q_h} = \frac{1-\xi}{\xi}. \tag{13}$$

Provided that this condition is satisfied, carriers will share the same temperature throughout the operation of the device only if the energy-selective contacts are positioned according to

$$\begin{cases} E_{\text{ext,e}} = \frac{E_g}{2} + (1-\xi)(E_{\text{ext}} - E_g) \\ E_{\text{ext,h}} = \frac{E_g}{2} + \xi(E_{\text{ext}} - E_g) \end{cases}, \tag{14}$$

where $E_{\text{ext}} = E_{\text{ext,e}} + E_{\text{ext,h}} > 0$ is a free parameter set by the design of the ESC. In the following, this situation where $E_{\text{ext,e}}$ and $E_{\text{ext,h}}$ satisfy Eq. (14) for any given E_{ext} will be referred to as "1T design."

If both conditions in Eqs. (13) and (14) are satisfied, the device will operate as a 1T HCSC at temperature $T = T_{\text{eff}} = T_e = T_h$ with a thermalization coefficient $Q = Q_e + Q_h$ and an energy-selective extraction $E_{\text{ext}} = E_{\text{ext,e}} + E_{\text{ext,h}}$.

3 Operation of a Two-Temperature Hot-Carrier Solar Cell

3.1 Voltage of a 2T HCSC

By definition, the voltage of a solar cell is the difference in the electrochemical potential of its terminals

$$eV = \mu_{e,\text{n contact}} + \mu_{h,\text{p contact}}, \tag{15}$$

where $\mu_{e,\text{n contact}}$ is the electrochemical potential of electrons in the n metallic contact and $\mu_{h,\text{p contact}} = -\mu_{e,\text{p contact}}$ is the chemical potential of holes in the p metallic contact. The "+" sign is because of our convention for hole energies (see Appendix A).

In a conventional solar cell, electrochemical potentials equilibrate between the absorber and the contacts, and the voltage is given by the QFLS in the absorber $eV = \Delta\mu$. By contrast, in a 1T HCSC, the isentropic extraction of carriers from the hot absorber toward the cold terminal through mono-energetic ESC leads to[1]

$$eV = \Delta\mu + \frac{E_{\text{ext}} - \Delta\mu}{T}(T - T_{\text{lattice}}), \tag{16}$$

where $\Delta\mu$ is the QFLS in the absorber.

Following the same derivation with $T_e \neq T_h$ (see Appendix B for further details), the voltage generated by a 2T HCSC can be expressed as

$$eV = \Delta\mu + \frac{E_{\text{ext,e}} - \mu_e}{T_e}(T_e - T_{\text{lattice}}) + \frac{E_{\text{ext,h}} - \mu_h}{T_h}(T_h - T_{\text{lattice}}). \tag{17}$$

This expression can be estimated in the specific case of the 1T design [i.e., if the ESC is located according to Eq. (14)] (note that, in the general case with arbitrary thermalization coefficients, $T_e \neq T_h$ even in the 1T design. $T_e = T_h$ requires the two conditions in Eqs. (13) and (14) to be satisfied). In this case,

$$eV = \Delta\mu_{\text{eff}} + \frac{E_{\text{ext}} - \Delta\mu_{\text{eff}}}{T_{\text{eff}}}(T_{\text{eff}} - T_{\text{lattice}}). \tag{18}$$

Remarkably, this expression does not depend on the temperature ratio r but only on the effective temperature and the effective chemical potential. The consequences of these properties will be discussed below.

3.2 Efficiency of a 2T HCSC

Combining the voltage expression 17 with the detailed balance model, it is possible to compute the J–V curve of the 2T HCSC device under a given illumination. The maximal power point is identified in the J–V curve, and the nominal power of the device is estimated as

$$P_{\text{out}} = JV_{\text{MPP}}. \tag{19}$$

Finally, the efficiency η is defined as the ratio between the output electrical power and the incident Sun power

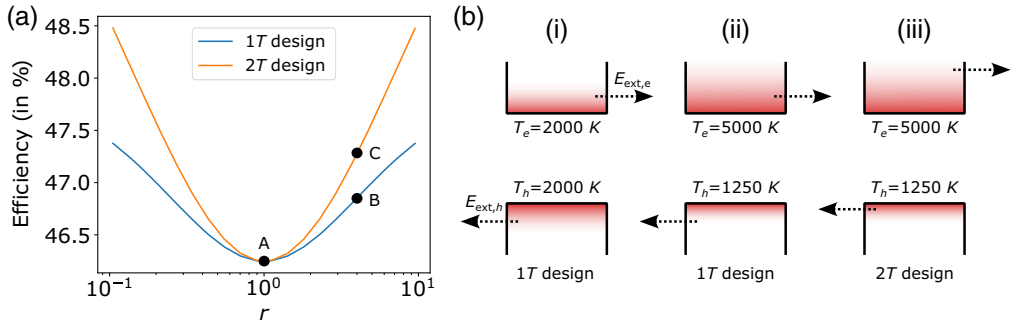

Fig. 2 (a) Efficiency of the 1T and 2T designs as a function of the temperature mismatch $r = T_e/T_h$. (b) Schematic representation of carrier temperatures and extraction energies in several cases: (i) $r = 1$ with the 1T design, (ii) $r = 4$ with the 1T design, and (iii) $r = 4$ with the optimal ESC design. This figure was computed for an absorber with $E_g = 1$ eV, $\xi = 1/2$, $T_{\text{eff}} = 2000$ K at V_{oc}, and $C = 1$.

$$\eta = \frac{P_{\text{out}}}{P_{\odot}(C)}. \tag{20}$$

4 Comparison Between 1T and 2T Hot-Carrier Solar Cell Efficiencies

To estimate the influence of $T_e \neq T_h$ on the operation of an HCSC, several situations will be compared in this section (see Fig. 2). This study does not aim to provide an exhaustive analysis and will be restricted to selected cases. In all cases considered below, the gap is taken to be $E_g = 1$ eV, the mass mismatch is $\xi = 1$ (i.e., $m_e = m_h$). Other configurations have also been tested (not shown here) and reached conclusions similar to those presented below.

The voltage analysis Eq. (18) has shown the importance of the effective temperature to parametrize the system. We will therefore consider systems with the same effective temperature $T_{\text{eff}} = 2000$ K at open-circuit voltage conditions but different temperature ratios $r = T_e/T_h$. Note that in the case presented here, the performances will be symmetric with respect to $r = 1$ because the effective masses are equal.

4.1 Reference 1T System

The reference point will be provided by the corresponding 1T HCSC—i.e., a system where the thermalization coefficients satisfy the condition in Eq. (13), such that $T_e = T_h = 2000$ K at V_{OC}, and the ESC satisfies the condition in Eq. (14). For this system, the maximal efficiency is achieved when $E_{\text{ext}} = 1.687$ eV and reaches an efficiency of 46.2%. This system corresponds to the situation A in Fig. 2.

4.2 2T HCSC with the Reference Contact Design

Let us now consider a 2T HCSC with the same ESC as the reference system but different thermalization coefficients such that $r \neq 1$ at V_{OC}. This system with $r = 4$ corresponds to the situation B in Fig. 2.

Remarkably, the power-conversion efficiency of this system is slightly increased compared with the reference situation, up to 1 point for large values of r. To further interpret this result, it may be insightful to identify the origin of this improvement by analyzing the usual electrical figures of merit.[11]

The 2T HCSC and the reference 1T HCSC absorb the same amount of solar radiation. In the detailed balance model Eq. (12), they will therefore reach the same short-circuit current.

At open-circuit voltage, particle balance enforces that the recombination rate is the same in the 2T HCSC and the reference situation. As the two systems share the same T_{eff}, Eq. (6) enforces that they also share the same $\Delta\mu_{\text{eff}}$. Finally, as the ESC of the 2T HCSC follows the 1T

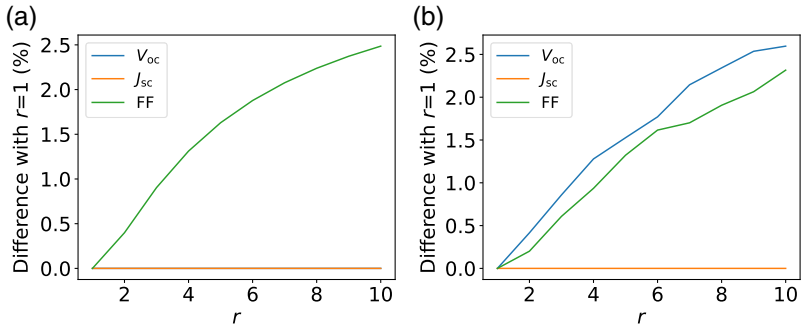

Fig. 3 Variation of the electrical figures of merit as a function of the temperature mismatch r for 2T HCSCs with (a) the 1T design and (b) the 2T design. As we consider the case $\xi = 1/2$, the case $r \leq 1$ is symmetrical of the case $r \geq 1$. This figure was computed for an absorber with $E_g = 1$ eV, $T_{\text{eff}} = 2000$ K at V_{oc}, and $C = 1$. Noise is due to poor convergence of the optimization algorithm.

design, Eq. (18) shows that 2T HCSC and the reference 1T HCSC will share the same open-circuit voltage.

The gain in power-conversion efficiency is therefore entirely due to an improvement of the fill factor. This result is numerically verified in Fig. 3(a).

4.3 2T HCSC with Optimal Contact Design

Finally, the absolute optimal power-conversion efficiency is estimated by optimizing the location of the ESC for each value of r. Such a system with $r = 4$ corresponds to situation C in Fig. 2.

This additional degree of freedom allows a further improvement of the power-conversion efficiency, up to two points above the reference value for large values of r.

A similar analysis of the electronic figures of merit as in the previous case can be performed. With the same argument as before, the short-circuit current is expected to remain independent of the contact design and the temperature ratio. By contrast, as the ESC position does not follow the 1T design anymore, Eq. (18) does not hold, and the more general solution [Eq. (17)] should be used. The open-circuit voltage can thus be increased compared with the 1T HCSC, and the efficiency improvement is therefore due to an increase of both the open-circuit voltage and the fill factor. This result is numerically verified in Fig. 3(b).

4.4 Discussion

Four main consequences can be drawn from the previous analysis.

First, for a given effective temperature, the temperature imbalance between electrons and holes is not detrimental to the HCSC operation. The efficiency decrease due to the lower temperature of one type of carrier is more than compensated by the efficiency increase due to the higher temperature of the other. This gain in efficiency is primarily due to an increased fill factor and possibly to an increased open-circuit voltage if the contact is adequately designed.

Second, the performance of an HCSC essentially depends on the effective temperature T_{eff} and is quite insensitive to temperature imbalance. The possible gain in efficiency is indeed limited—less than 2 points for very large temperature ratios with optimized ESC. This property can be seen as the robustness of the HCSC system[15]: even if the system does not operate exactly in nominal conditions, it is able to maintain a performance close to the nominal value.

A corollary of this point is that the knowledge of the effective temperature T_{eff} is sufficient to design a satisfying ESC of a 2T HCSC by considering the 1T design at the same temperature. This design will not be optimal for the 2T system but will be close enough to the optimum to allow efficiencies less than 1 point below the maximal value.

Finally, photoluminescence (PL) is confirmed as an adequate tool for the investigation of hot-carrier solar cells. Although a refined analysis is required to discriminate T_e from T_h in the band-filling signature of the PL signal,[5] the effective temperature T_{eff} actually yields the minimal information required to design the ESC of a 2T HCSC. Considering the spectral distribution of the PL emission Eq. (6), this quantity can be measured with simpler methods ranging from high-energy linear fit[16,17] to full fit analyses.[18,19]

5 Conclusion

A model for a HCSC with $T_e \neq T_h$ has been derived by introducing different thermalization coefficients for electrons and holes in a simple detailed model approach. The temperature imbalance has consequences on the radiative emission of the cell and the voltage generated at its terminals. This model has been used to simulate the operation of a 2T HCSC and compare its performance to a reference 1T HCSC. This analysis shows the robustness of HCSC against uneven temperatures and underlines the importance of the effective temperature T_{eff}. Surprisingly, a temperature imbalance at a fixed effective temperature leads to a slight power-conversion efficiency increase primarily due to an improvement of the device's fill factor.

In this work, electrons and holes were assumed to have homogeneous (and different) temperatures throughout the absorber. Complementarily, carriers could be assumed to share the same temperature, but this temperature could vary spatially. Such a thermoelectric-like situation could for instance arise from an inhomogeneous distribution of the absorbed power in the depth of the device if the heat transport is too limited to homogenize temperatures.[20,21] In this case, carriers would be colder at one contact and hotter at the other contact. Modeling this situation would require several modifications to the current model, but the expression for the 2T voltage Eq. (17) would remain valid, considering the temperature of each type of carrier at the contact where they are extracted.

The simple model presented here could be refined by including energy exchange between electron and hole populations. This interaction would tend to equate carrier temperatures, reducing the value of r reached for given thermalization coefficients. It would therefore further reduce the influence of the effects reported here, reinforcing the conclusion that T_{eff}, which can be accessed through PL measurements, is the main factor governing the achievable power-conversion efficiency of an HCSC.

6 Appendix A: Energy Convention

Following the sign convention introduced in Ref. 4, the energy of holes in the valence band is counted negatively, as shown in Fig. 4. The origin of energy is taken at mid-gap.

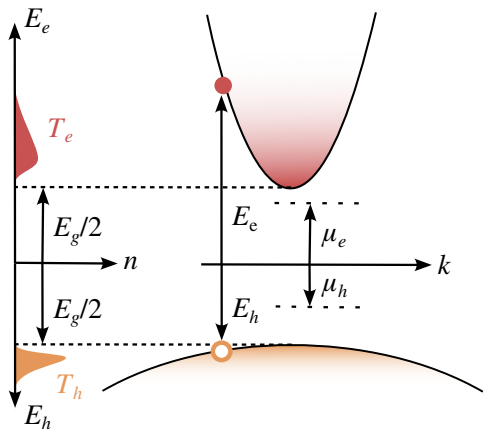

Fig. 4 Energy conventions used in this work are similar to those of Ref. 4. We represent the case of a semiconductor with parabolic bands under illumination. Color gradients represent the occupation of each band. Carrier densities are represented on the vertical left axis. We represent here a case where holes are colder than electrons. By convention, the energy axis is reversed of holes. This means that positive quantities for electrons are denoted by upward arrows, whereas they are denoted by downward arrows for holes.

7 Appendix B: Detailed Derivation of the 2T HCSC Voltage

To compute the voltage of a 2T HCSC, we assume that electrons and holes are described by thermal distributions, characterized by T_e, μ_e, T_h, and μ_h. These four variables form the thermodynamical state of the absorber. By convention, electrons are extracted at the right contact (at room temperature and with a chemical potential $\mu_{e,R}$), and holes are extracted in the left contact (with chemical potential $\mu_{h,L}$). Note that the latter process is equivalent to reinjecting electrons in the absorber from the left contact, with a chemical potential $\mu_{e,L} = -\mu_{h,L}$.

The voltage of an electrical device V is linked to the work that one can extract from an electron circulating across the system. By definition, this is linked to the chemical potential of the electrodes as

$$eV = e\frac{P_{\text{elec}}}{J} = \mu_{e,n\,\text{contact}} + \mu_{h,p\,\text{contact}}. \tag{21}$$

By writing the thermodynamical equilibrium of the 2T HCSC, it is possible to compute $\mu_{e,n\,\text{contact}}$ and $\mu_{h,p\,\text{contact}}$ as a function of the thermodynamical state in the absorber. We write the variation of energy in the absorber, dU_e^{abs}, and in the contact dU_e^{con} at the right side of the system, where an electron is removed from the absorber and injected in the contact. By definition,

$$\begin{cases} dU_e^{\text{abs}} = -E_{\text{ext,e}} = -\mu_e + T_e dS_e^{\text{abs}} \\ dU_e^{\text{con}} = +E_{\text{ext,e}} = +\mu_{\text{e,n contact}} + T_{\text{lattice}} dS_e^{\text{con}} \end{cases}, \tag{22}$$

where

$E_{\text{ext,e}}$ is the extraction energy of electrons at the right contact.

μ_e is the chemical potential of electrons in the absorber.

T_e is the temperature of electrons in the absorber.

T_{lattice} is the temperature of carriers in the contact. In general, we assume that $T_{\text{lattice}} = 300$ K.

dS_e^{abs} is the variation of entropy in the absorber at the right contact.

dS_e^{con} is the variation of entropy in the right contact.

Similarly, at the left contact, where an electron is injected from the contact to the absorber (i.e., a hole is injected from the absorber valence band to the contact valence band), one gets

$$\begin{cases} dU_h^{\text{abs}} = -E_{\text{ext,h}} = -\mu_h + T_h dS_h^{\text{abs}} \\ dU_h^{\text{con}} = +E_{\text{ext,h}} = +\mu_{\text{h,p contact}} + T_{\text{lattice}} dS_h^{\text{con}} \end{cases}, \tag{23}$$

where the signs of $E_{\text{ext,h}}$, μ_h, and $\mu_{\text{h,L}}$ have been changed because we describe electrons in the valence band as holes with opposite energy and chemical potential (see Appendix A).

As the exchange of particles is supposed to be isentropic, no entropy is created in the system, such that

$$dS^{\text{abs}} + dS^{\text{con}} = 0 \quad \Leftrightarrow dS_e^{\text{abs}} + dS_h^{\text{abs}} = -dS_e^{\text{con}} - dS_h^{\text{con}}. \tag{24}$$

By injecting Eqs. (22) and (23), we obtain

$$\frac{\mu_e - E_{\text{ext,e}}}{T_e} + \frac{\mu_h - E_{\text{ext,h}}}{T_h} = -\frac{E_{\text{ext,e}} - \mu_{\text{e,n contact}} + E_{\text{ext,h}} - \mu_{\text{h,p contact}}}{T_{\text{lattice}}}, \tag{25}$$

$$\Leftrightarrow eV = E_{\text{ext,e}}\left(1 - \frac{T_{\text{lattice}}}{T_e}\right) + \mu_e \frac{T_{\text{lattice}}}{T_e} + E_{\text{ext,h}}\left(1 - \frac{T_{\text{lattice}}}{T_h}\right) + \mu_h \frac{T_{\text{lattice}}}{T_e}, \tag{26}$$

$$\Leftrightarrow eV = \Delta\mu + \frac{E_{\text{ext,e}} - \mu_e}{T_e}(T_e - T_{\text{lattice}}) + \frac{E_{\text{ext,h}} - \mu_h}{T_h}(T_h - T_{\text{lattice}}). \tag{27}$$

Disclosures

No conflicts of interest, financial or otherwise, are declared by the authors.

Code and Data Availability

The 2T HCSC model described in this article was implemented in Python code and has been released on GitHub in a private repository. It can be made available upon request to the corresponding author.

Acknowledgments

This work was supported by the French National Research Agency under the grant ANR GELATO (Grant No. ANR-21-CE50-0017) and the PEARL program at Institut du Photovoltaïque d'Ile de France (IPVF).

This work was supported by the French National Research Agency under the grant ANR ICEMAN (Grant No. ANR-19-CE05-0019-01) and GELATO (Grant No. ANR-21-CE50-0017) and the PEARL program at Institut du Photovoltaïque d'Ile de France (IPVF).

References

1. R. T. Ross and A. J. Nozik, "Efficiency of hot-carrier solar energy converters," *J. Appl. Phys.* **53**, 3813–3818 (1982).
2. P. Wurfel, "Solar energy conversion with hot electrons from impact ionisation," *Sol. Energy Mater. Sol. Cells* **46**, 43–52 (1997).
3. P. Wurfel, "The chemical potential of radiation," *J. Phys. C: Solid State Phys.* **15**, 3967–3985 (1982).
4. F. Gibelli, L. Lombez, and J.-F. Guillemoles, "Two carrier temperatures non-equilibrium generalized Planck law for semiconductors," *Phys. B Condens. Matter* **498**, 7–14 (2016).
5. T. Vezin et al., "Direct determination of electron and hole temperatures from continuous-wave photoluminescence measurements," *Phys. Rev. B* **110**, 125207 (2024).
6. F. Gibelli, L. Lombez, and J.-F. Guillemoles, "4—Hot-carrier solar cells: modeling carrier transport," in *Advanced Micro- and Nanomaterials for Photovoltaics*, D. Ginley and T. Fix, Eds., Micro and Nano Technologies, pp. 53–92, Elsevier (2019).
7. W. Shockley and H. J. Queisser, "Detailed balance limit of efficiency of p-n junction solar cells," *J. Appl. Phys.* **32**(510), 11 (1961).
8. J.-F. Guillemoles et al., "Guide for the perplexed to the Shockley–Queisser model for solar cells," *Nat. Photonics* **13**, 501–505 (2019).
9. A. Le Bris et al., "Étude de faisabilité de dispositifs photovoltaïques à porteurs chauds: conception, modélisation, caractérisation," [PhD thesis] (2011).
10. M. Giteau et al., "Detailed balance calculations for hot-carrier solar cells: coupling high absorptivity with low thermalization through light trapping," *EPJ Photovolt.* **10**, 1 (2019).
11. P. Wurfel and U. Wurfel, *Physics of Solar Cells: From Basic Principles to Advanced Concepts*, 3rd ed., Wiley-VCH Verlag GmbH & Co. KGaA, Weinheim (2016).
12. A. Le Bris et al., "Thermalisation rate study of GaSb-based heterostructures by continuous wave photoluminescence and their potential as hot carrier solar cell absorbers," *Energy Environ. Sci.* **5**(3), 6225–6232 (2012).
13. H. Esmaielpour et al., "Impact of excitation energy on hot carrier properties in InGaAs multi-quantum well structure," *Prog. Photovolt. Res. Appl.* **30**(11), 1354–1362 (2022).
14. A. Le Bris and J.-F. Guillemoles, "Hot carrier solar cells: achievable efficiency accounting for heat losses in the absorber and through contacts," *Appl. Phys. Lett.* **97**, 113506 (2010).
15. M. Giteau et al., "Hot-carrier multijunction solar cells: sensitivity and resilience to nonidealities," *J. Photonics Energy* **12**, 032208 (2022).
16. J. Shah and R. C. C. Leite, "Radiative recombination from photoexcited hot carriers in GaAs," *Phys. Rev. Lett.* **22**, 1304–1307 (1969).
17. R. A. Höpfel, J. Shah, and A. C. Gossard, "Nonequilibrium electron-hole plasma in GaAs quantum wells," *Phys. Rev. Lett.* **56**, 765–768 (1986).
18. D.-T. Nguyen et al., "Quantitative experimental assessment of hot carrier-enhanced solar cells at room temperature," *Nat. Energy* **3**, 236–242 (2018).
19. H. Esmaielpour et al., "Investigation of hot carrier thermalization mechanisms in quantum well structures," *Proc. SPIE* **11681**, 116810N (2021).
20. S. Limpert et al., "Bipolar photothermoelectric effect across energy filters in single nanowires," *Nano Lett.* **17**, 4055–4060 (2017).
21. T. Vezin et al., "Optical determination of thermoelectric transport coefficients in a hot-carrier absorber," *Phys. Rev. Appl.* **22**, 034018 (2024).

Thomas Vezin has a PhD in physics and is specialized in high efficiency photovoltaics. He conducts fundamental research on energy conversion, with interests in photovoltaics,

photoluminescence, thermoelectricity and charge transport in semiconductors. He took part in the SolairePV initiative, a collective work aiming at assessing photovoltaics strengths and weaknesses in the energy transition to come in France.

Nathan Roubinowitz is currently a PhD student at the IPVF, he hold an master's degree from ENS Paris-Saclay in fundamental physics. His studies focused on theoretical condensed matter physics, including a research internship in superconductivity. Subsequently, he transitioned to applied physics, concentrating on photovoltaics.

Jean François Guillemoles is a CNRS research director, head of the IPVF joint lab (between CNRS, IPP, PSL and SAS IPVF) in Palaiseau (France) aiming at the development of photovoltaics, and a former director of NextPV, a joint lab with the University of Tokyo and part time professor at Ecole Polytechnique. He is a author/co-author of more than 450 publications (peer-reviewed papers, book chapters, patents, proceedings, etc.), editor for Progress in Photovoltaics and director of several large R&D programs. His research topics on solar energy: high efficiency concepts, new applications, luminescence-based characterization techniques, and modeling of materials and devices.

Daniel Suchet is a professor at École Polytechnique and a researcher at Institut du Photovoltaïque d'Île de France (IPVF), Palaiseau, France. He received his engineering degree from École Polytechnique in 2014 and prepared his PhD on ultracold atoms at the Laboratoire Kastler Brossel in Paris. He then turned to solar energy at NextPV (University of Tokyo, Japan), and is currently working on thermodynamics and advanced characterization for solar energy conversion.